Crystal facet engineering in Ga-doped ZnO nanowires for MIR plasmonics.

Vincent Sallet, Corinne Sartel, Said Hassani, Christèle Vilar, Gaelle Amiri, Alain Lusson, François Jomard, Pierre Galtier, Isabelle Lefebvre, Christophe Delerue, et al.

Crystal facet engineering in Ga-doped ZnO nanowires for MIR plasmonics

Vincent Sallet[1], Corinne Sartel[1], Said Hassani[1], Christèle Vilar[1], Gaelle Amiri[1], Alain Lusson[1], François Jomard[1], Pierre Galtier[1], Isabelle Lefevbre[2], Christophe Delerue[2], Mohamed K. Hamza[3], Bruno Canut[3], Bruno Masenelli[3].*

[1] Université Paris-Saclay, CNRS, Université de Versailles St Quentin en Yvelines, 45 avenue des Etats-Unis, Groupe d'Etude de la Matière Condensée (GEMAC), 78035 Versailles, France

[2] Université de Lille, CNRS, Centrale Lille, ISEN, Université de Valenciennes, UMR 8520-IEMN, 59000 Lille, France

[3] Institut des Nanosciences de Lyon (INL-UMR5270), Université de Lyon, INSA-Lyon, ECL, UCBL, CPE, CNRS, 69621 Villeurbanne, France

KEYWORDS

ZnO, nanowires, surfactant, doping, crystal facets, plasmonics

ABSTRACT

The MOCVD growth of various Ga-doped ZnO nanostructures for plasmonics is investigated, with a particular focus on the nanowire facet transformations induced by the addition of trimethylgallium in the gas phase. For non-intentionally doped spontaneous ZnO nanowires, the aspect ratio is strongly decreased due to residual Ga in the reactor, and the shape evolves rapidly towards Christmas-tree like and hierarchical structures upon intentional Ga doping. Regarding ZnO/ZnO:Ga core-shell structures, a change of the smooth initial M-oriented facets occurs, with the development of {20-21} surfaces, and further {10-11} and {0001} surfaces. Interestingly, a similar evolution of the lateral roughness is observed in Au-catalyzed doped nanowires. High concentrations of Ga in the grown nanostructures are revealed by photoluminescence and confirmed by Rutherford backscattering spectrometry. First photoacoustic measurements show an optical absorption at 6 μm, evidencing that the degenerated material is suitable for plasmonics applications in the IR range. The influence of Ga doping on the facet transformations and the occurrence of unexpected {0001} polar surfaces are discussed. The results can be mainly understood by a Ga surfactant effect (at least partial) responsible for the modification of the surface energies and kinetics. Density functional calculations support the floating behavior of the negatively charged Ga^- ion on the growing surface.

1. INTRODUCTION

Semiconductor nanowires have already demonstrated enormous potential for future generations of electronic and optoelectronic nanodevices. For now more than a decade, silicon and III-V compounds (GaN, GaAs…) based nanostructured demonstrators have shown to improve the performances of a variety of devices such as transistors, LEDs, sensors, solar cells, and have

opened the way to new types of nanogenerators based on piezoelectric nanowires (NWs) [1,2,3]. Semiconductor nanostructures made of II-VI materials are also attractive, in particular ZnO nanowires which can be easily grown using industrial and low-cost techniques. ZnO offers a tremendous combination of physical properties such as a wide direct bandgap, large exciton binding energy, piezoelectric properties, biocompatibility... Heavily doped, ZnO acts as a degenerate semiconductor and offers the possibility to extend the plasmon wavelength of metals (limited to the visible range) to the IR range, including the telecom wavelengths. In this research field, gallium-doped ZnO layers and nanoparticles have been proposed [4,5,6]. According to the Drude model, the resonance of plasmonic waves can be controlled by tuning the free carrier concentration, offering new opportunities in the Mid IR range. This paves the way to an enhanced detection of molecules (gas sensors), if the absorption wavelength is resonant with the plasmon wavelength. Besides, the architecture of nanowires exhibiting a high aspect ratio is particularly interesting for the latter application [7].

In this study, we are interested in heavily Ga-doped ZnO nanowires (GZO-NWs), in the aim to reach very high carrier concentrations suitable for IR plasmonic applications. Degenerate ZnO nanowires represent an interesting alternative to ITO ones, using more abundant and less toxic materials. Nevertheless, doping ZnO NWs with control of both impurity concentration and NW morphology (*i.e.* axis direction, facet orientations, aspect ratio…) is an important issue, since *in situ* doping is expected to strongly affect the growth process. Indeed, as far as semiconductor growth is concerned, many papers report on crystal facet transformations, surface roughness or nanostructure shape evolutions with the addition of a dopant or a foreign element in the gas/liquid phase [8,9,10]. Most often the term "surfactant" is used to label the observed phenomenon, and the consequence is that, in the literature, this commonly evoked "surfactant effect" covers a wide range

of growth mechanisms. Intentionally added in the gas phase with the source precursors, a surfactant element is usually described by a low vapor pressure and a low solubility in the growing material, resulting in a surface accumulation, and thus modifying thermodynamics and kinetics at the growth front. In solution growth, the surfactant effect is also intensively used for the realization of ZnO flower like structures [11,12].

This work focuses on the transformation of the facets of ZnO nanostructures upon *in situ* Ga doping, *i.e.* adding metalorganic molecules of Ga in the gas phase during the growth of ZnO nanowires. The structural properties and orientation of the newly formed facets are thoroughly investigated by scanning and transmission electron microscopies. Surprisingly, polar surfaces, which are believed to be energetically not favorable, appear in the new growth process, leading to "skewer-like" morphologies. The incorporation of Ga in the grown samples is assessed by energy dispersive X-ray spectroscopy (EDS), Rutherford backscattering spectrometry (RBS), and photoluminescence. With the help of density functional calculations, the transformation of the morphologies is discussed in terms of thermodynamics, kinetics and surfactant effects.

2. METHODOLOGY

2.1 Experimental

Three kinds of Ga-doped ZnO one dimensional (1D) nanostructures were grown by using metalorganic chemical vapor deposition (MOCVD) : i) spontaneous Ga-doped ZnO NWs grown without any catalyst, ii) core/shell ZnO/ZnO:Ga structures, and iii) catalyst-assisted (gold droplet) Ga-doped ZnO NWs. Samples were grown in a horizontal quartz reactor operating at low pressure (50 torr) and allowing high growth temperature up to 1000°C. Diethylzinc (DEZn) and trimethylgallium (TMGa) were used as metalorganic sources. Growths have been performed at

875-1000°C using nitrous oxide (N_2O) as oxygen source. Carrier gas was helium. Table 1 details the growth parameters for each kind of GZO nanostructure.

Sample	Structure type	Tg	Growth time	DEZn flow (µmol/min)	N_2O flow (µmol/min)	TMGa flow (µmol/min)	substrate
S1	Spontaneous	875°C	30 min	40	32000	0 (clean reactor)	
S2	NWs			40	32000	0 (residual Ga)	Sapphire
S3				40	32000	0.03	
S4				40	32000	0.3	
CS1	Core/shell	900°C	5 min	20	108000	0.03	Sapphire +
CS2			20 min	20	108000	0.03	ZnO NWs
Cat1	Catalyst-	1000°C	20 min	40	32000	0	Silicon + Au
Cat2	assisted NWs			40	32000	0.22	droplets
Cat3				40	32000	0.88	

Table 1. MOCVD conditions used for ZnO:Ga nanostructures growth

The morphology has been assessed by scanning electron microscopy (SEM, JEOL 7001). Transmission electron microscopy (TEM) analysis was carried out using a TOPCON 002B microscope operating at 200 kV, and equipped with energy dispersive X-ray spectroscopy. For optical measurements, photoluminescence experiments have been carried out at 5K using the 351 nm UV line of an argon ion laser. In addition, the photoacoustic signals from several samples have been recorded using the IR source of a Brucker Vertex V80 FTIR and the PA301 detector from Gasera Inc.

Complementary characterization was obtained using Rutherford backscattering spectrometry (RBS) in order to measure the doping level of gallium. The analysis was performed with $^4He+$ ions of 3.3 MeV energy delivered by the 4 MV Van de Graaff accelerator of the Nuclear Physics Institute of Lyon (IPNL). With the help of the SIMNRA simulation code [13] we extracted from the experimental data the average stoichiometry [Ga]/[Zn] within an uncertainty estimated at ± 0,5%.

Secondary ion mass spectroscopy (SIMS) cannot process nanowires, but was used to measure the Ga concentration of reference 2D layers. The latter were also grown by MOCVD in the same reactor, using similar conditions (temperature, pressure, TMGa flow) but using high oxygen/zinc ratio ($R_{VI/II}$), which causes the transition from 1D growth to 2D [14]. Without stating that the Ga incorporation is equivalent in nanowires and in layers, these measurements can however give an idea of the doping levels involved in this study.

2.2 Theoretical

Structure relaxations and formation energies were computed within the DFT framework. Our calculations were performed using the projector augmented wave (PAW) method [15] as implemented in the VASP code [16]. Details are given in the supporting information.

3. RESULTS AND DISCUSSION

3.1 Structural characterization of undoped and Ga-doped ZnO NWs

Figure 1 gathers SEM images of undoped and Ga-doped ZnO NWs spontaneously grown on sapphire. For the undoped sample shown in figure 1a, it is important to note that the growth was performed prior to any introduction of Ga precursor into the MOCVD system, *i.e.* in a reactor where we do not expect any Ga contamination. In that case, ZnO NWs raise vertically along [0001] C axis on the top of ZnO pyramids. Lateral facets of the nanowires are non polar (10-10) M-oriented planes. Length is around 6 µm and diameter is near 100 nm. This kind of ZnO nanostructures has been commonly observed in the literature and is typical of high temperature MOCVD growth [17, 18]. As a function of the growth parameters, the length and diameter can be easily tuned in the range [1-10 µm] and [30nm-500nm], respectively, but not independently,

anyway. It has been published that ZnO NWs grow along [0001] Zn-polar (called +C) direction after polarity inversion on the top of [000-1] O-polar (called-C) oriented ZnO pyramids [19]. Figure 1b shows the morphology of ZnO NWs which were not intentionally doped (TMGa flow=0sccm) but elaborated after a series of doping experiments, *i.e.*, in conditions where a Ga pollution may occur from injection lines and/or reactor inlet. Compared to the previous sample, the length is much reduced to ~2 µm, and the diameter is increased to ~400 nm. This clearly indicates an enhancement of the radial growth rate at the expense of the axial growth rate. RBS measurements could not detect any Ga contribution, which is below the detection limit of 0.5%. Nevertheless, the residual Ga doping in the material could be estimated around a few 10^{17} at.cm^{-3}, from SIMS characterization of ZnO 2D layers which were neither intentionally doped, but grown with similar conditions.

Intentional doping with TMGa flows makes the morphology drastically evolve. With 0.03 µmol/min TMGa flow, sharp GZO cones and "Christmas-tree" shaped structures are produced, as seen in figure 1c. This observation gives evidence of a modification of the lateral growth and, more specifically, of the facets orientation. In the case of 2D film growth, such a doping level leads to a Ga concentration around 10^{19} at.cm^{-3} as measured by SIMS. Going further, high level of Ga-doping (0.3 µmol/min) induces the formation of a hierarchical nanostructure where multiple growths of ZnO branches initiate and develop on previously formed tree-like structures. Such hierarchical structures are expected to be of great interest for environmental applications [20]. RBS measurements have been carried out and indicate a Ga concentration of 2% ± 0.5%. By using SIMS, Ga concentration is measured above 10^{20} at.cm^{-3} in the reference 2D grown GZO.

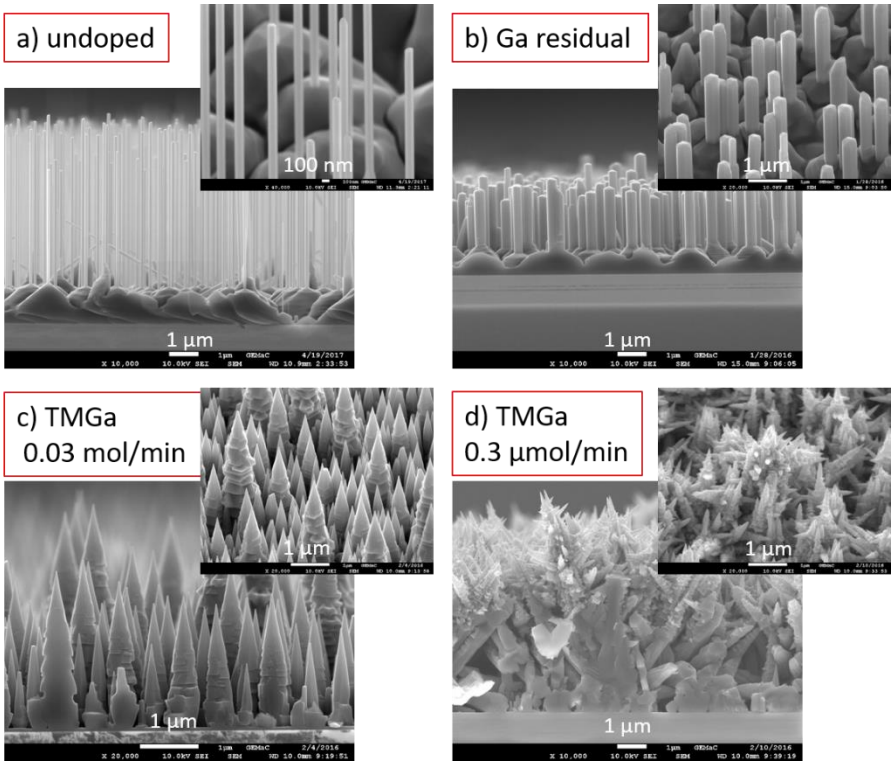

Figure 1. SEM images of ZnO nanowires : a) undoped and clean reactor, b) non intentionally doped by residual Ga in the reactor, c) doped with 0.03µmol/min TMGa flow, d) doped with 0.3µmol/min TMGa flow

3.2 Structural characterization of ZnO/ZnO:Ga core-shell NWs

ZnO/ZnO:Ga core-shell structures have been synthesized in order to more specifically study the lateral growth of GZO on M-plane facets. Figure 2 shows SEM images of two samples for which a Ga-doped ZnO shell (TMGa=0.03 µmol/min) has been deposited on previously-grown undoped ZnO NWs (such as in figure 1a), with a growth duration of 5 and 20 minutes, respectively. A 5 min growth produces a thickness of approximately 10 nm (estimated from the difference between the sole core and the core/shell structure diameters) and leads to a significant roughness of the facets. As it can be observed on TEM images (figure 2b), this roughness corresponds to the

development of ZnO planes inclined at an angle of 15° relative to the initial M plane, and attributed to {20-21} planes. High resolution TEM image shows a continuity of the (0001) atomic plane between the ZnO core and the doped shell, evidencing a homoepitaxial growth. No extended crystal defects such as dislocations or stacking faults could be distinguished. EDS characterization does not detect any Ga, meaning that its concentration in the shell is below the detection limit of 0.5%. After 20 min deposition, the lateral roughness has drastically evolved and the morphology appears like a stacked bunch of ZnO nanoplates, like a "skewer" (figure 2c and 2d). These unusual nanoplates exhibit triangular or parallelepipedic shapes.

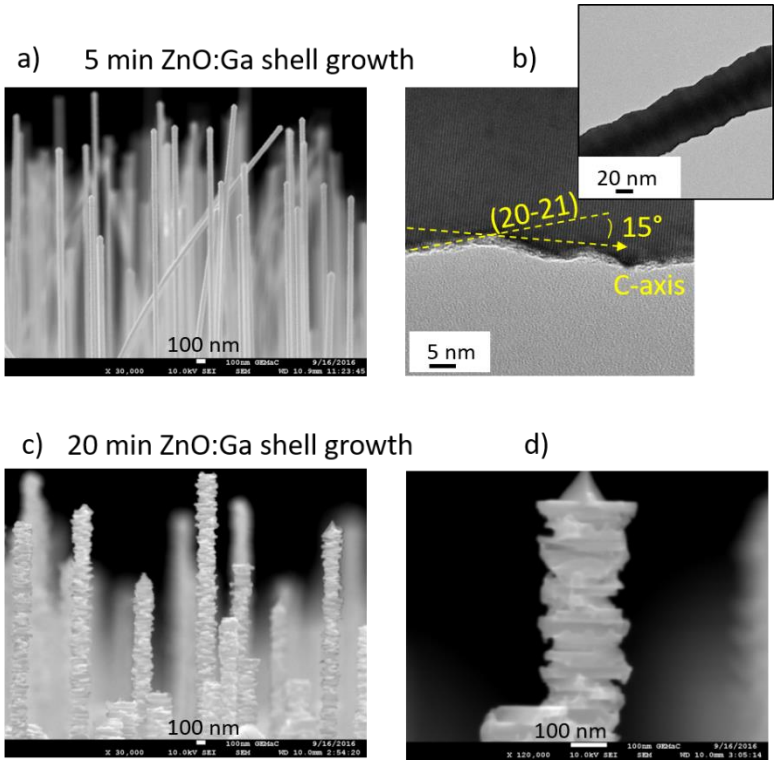

Figure 2. ZnO/ZnO:Ga core shell structures : a) SEM image of 5 min shell growth, b) TEM images of 5 min shell growth, c) and d) : SEM images of 20 min shell growth

We thus conclude, from the analysis of these first two series of samples, that Ga atoms on the growing surface strongly modify the nanowire axial growth along C-axis, as well as the development of the lateral facets. The effect is significant even at low Ga concentrations in the gas phase. For spontaneous GZO nanowires grown on sapphire, the more we increase TMGa precursor flow, the more transformed the initial 1D morphology is. It evolves progressively from shorter and bigger nanowires (residual Ga), to conical NWs (0.03µmol/min), and finally hierarchical structures (0.3 µmol/min). In core-shell ZnO/ZnO:Ga structures, we also expect a continuous transformation of the doped shell with the growth time. As the growth proceeds, the lateral roughness develops in such a way that the initial smooth M-plane facets of the core are finally changed to a stack of ZnO slices.

3.3. Structural characterization of Ga-doped Au-catalyzed NWs

In this work, we have also considered another mean of growing semiconductor nanowires, namely catalyst-assisted growth, where metallic droplets (*e.g.* gold droplets) are previously deposited on the surface to trigger the one-dimensional growth [21,22]. The method is also called VLS for vapor-liquid-solid or VSS for vapor-solid-solid depending on the involved mechanism. The catalyst is not necessary in the case of ZnO since nanowires can emerge spontaneously. However, it can be interesting to investigate the doping efficiency, *i.e.*, to assess whether the metallic droplet could force the incorporation of high concentrations of dopants.

We observed that the transformation of the morphology of catalyzed GZO NWs is very similar to the case of ZnO/ZnO:Ga core/shell structures, suggesting that the lateral growth mechanisms could be the same. Looking from the tip to the bottom of the NW, the morphology of the lateral facets evolves and shows first the appearance of {20-21} surfaces inclined at 15°, and subsequently

{10-11} surfaces which are inclined at an angle of 28° relative to the (10-10) M plane. Finally, the lower half part of the catalyzed NWs exhibits the previously observed stacking of ZnO nanoplates with C-oriented surfaces.

For the sake of clarity, the detailed experimental results are given in the Supporting information part.

3.4 Interpretation

Illustration of the facet transformation

These results, collected from different types of GZO nanostructures, reveal that upon Ga doping and under the MOCVD growth conditions described in the experimental part, the usual (10-10) M-plane cannot act as a growth front. Incoming Zn and O atoms incorporate on the lateral surfaces and develop other orientations of the facets due to the presence of adsorbed Ga atoms. Indeed, this is surprising since scanning tunneling microscopy (STM) has shown smooth and stable ZnO M-surfaces with well-defined terraces, even at high temperature (750°C) [23]. M-facets are expected to be preferred stable surfaces for ZnO nanostructured crystals.

It is interesting to look into the details of the crystalline structure of the ZnO (10-10) M-surface which is illustrated in figure 3. In particular, it is noticeable that zinc (oxygen) atoms are organized along lines in the [11-20] direction. These lines of Zn and O atoms are thus perpendicular to the [0001] C-direction. Interestingly, one must notice that the development of the lateral roughness shown in core-shell NWs and Au-Catalyzed NWs follows a rotation of the initial M-surface around these Zn (or O) lines and towards C-axis, as illustrated in figure 3. Upon Ga doping, the growth

front is tilted. Therefore, our observations are consistent with a progressive increase of the rotation angle between the initial M-plane and the newly formed growth front:

(10-10) M-plane => (20-21) at 15° relative to M => (10-11) at 28° => (0001) at 90°

This observation has to be taken into account if we try to understand the effect of Ga atoms on the growing surface. In a first analysis, a very simple model can be suggested as follows. Ga atoms are expected to incorporate on zinc site, so that their possible influence on the growth (*e.g.* passivation effects, exchange mechanism with newly incoming Zn…) will be extended along these lines. In figure 3, a hypothetical case is illustrated where the Ga atom replacing zinc may produce a step edge in the growth and induces the formation of a (20-21) plane which could later (or upon higher Ga doping) evolve towards (10-11) and (0001) planes. However, the exact mechanism can be more complex and is worth being discussed in light of our knowledge of surfactant effects.

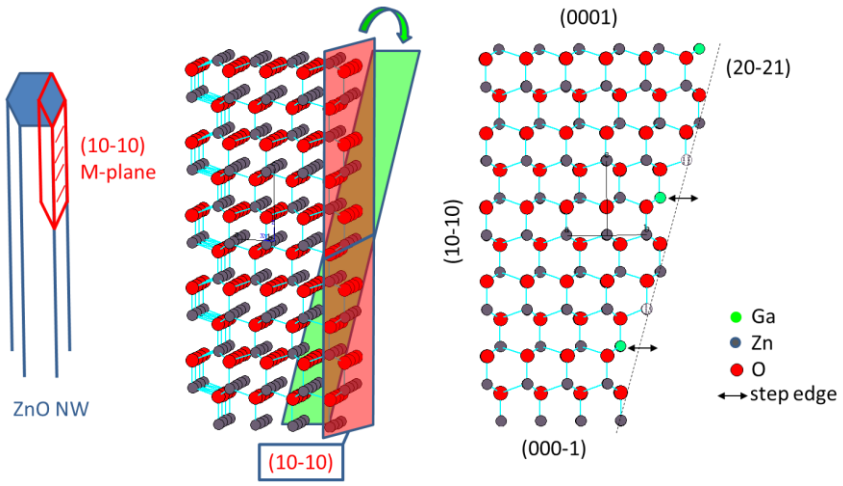

Figure 3. Illustration of the rotation of the initial M-plane facet around A-direction to form a (20-21) facet

Surfactant effects

As we already mentioned in the introduction part, the term "surfactant effect" is commonly used to describe the morphology transformation of semiconductor layers or nanostructures induced by dopant atoms or impurities. Precisely, surfactants lower the surface energy as well as modify the diffusion length of adsorbed atoms [24]. In particular, an exchange process occurs between the foreign atom and a newly incoming atom (of the material to be deposited) since it is more energetically favorable for the surfactant to float on the surface than to be buried and incorporated in the film. The main benefits of the surfactant effect have been to increase the critical thickness of strained films (*e.g.* SiGe layers on Si [25]), to favor layer-by-layer growth [26], and to prevent the growth mode transition from 2D to 3D, such as in the case of InGaAs(Sb) quantum wells [27]. However, the important literature on the topic tends to demonstrate that foreign atoms on the surface may induce a variety of thermodynamics and kinetics effects on the growth. Indeed, other mechanisms or complementary mechanisms to the surfactant effect have been proposed to explain morphology transitions observed in doped semiconductor nanostructures. In particular, the passivation of some surfaces that hinders the growth was reported. For example it has been shown that introducing silane, a SiN layer forms on the lateral facets of GaN NWs [28], and therefore the growth only proceeds on the topmost facet. The passivation effect of the lateral surfaces of GaSb NWs by using sulfur has also been reported [29]. Moreover, adatoms mobility has been discussed by Zhang *et al.* [30] during the growth of Sb-doped GaN, where Sb was observed to act as a surfactant. The influence of Sb is understood as a reduction of the N coverage at the surface, and thus a reduction of the V/III ratio which modifies the growth front and facets.

In this work, we do not observe a "classical" surfactant effect, in the sense of enhancing layer-by-layer growth and prohibiting 3D islands, but, contrary to the case of SiGe, we find a

morphology transition from 2D to 3D in the lateral growth on ZnO NWs facets. It is often expected that a surfactant will smoothen the surface. However, with the modification of thermodynamics and kinetics, various behaviors can be observed. For example in Voigtländer's article [31], it is reported that As and Sb on Si surface decrease the diffusion length of Si atoms during homoepitaxial growth and suppress 3D islanding in Ge/Si heteroepitaxy, whereas indium on the surface enhances the Si diffusivity and keeps 3D islanding. In our case, Ga atoms likely modify the surface energies as well as the kinetics at the growth front, favoring other orientations than the typical {10-10} M surfaces of undoped ZnO nanowires, and leading to the development of alternative lateral facets.

Occurrence of polar surfaces

Moreover, in this study, the most puzzling result is the emergence of (0001) and/or (000-1) facets. (0001) and (000-1) are polar surfaces and have a dipole moment in each periodic unit that generates an electric field perpendicular to the surface [32,33,34]. The theoretical ionic model [35] shows that the energy of the dipoles diverges, making theses surfaces unstable. Such clean and unreconstructed surfaces should not exist in grown ZnO crystals. In this context, the stabilization mechanism of (0001) and (000-1) polar ZnO surfaces has been controversial for many years. It requires rearranging the surface charge, *i.e.,* a reduction of the positively charged Zn surface, as well as the negatively charged O-surface [36]. This could be achieved by a charge transfer from the Zn to the O surface [37], (1x3) surface reconstruction [38], or hydroxylation of the surface [39]. The STM experiments of Dulud *et al.* [40] have shown an unreconstructed (1x1) Zn-polar ZnO surface exhibiting triangular holes and O-terminated step edges which reduce the surface Zn concentration. More recently, Lauritsen *et al.* [41] have found honeycomb structures by scanning probe microscopy on O-polar ZnO surface. Charged adsorbates may also stabilize a polar surface. Yuan

et al. [42] have reported a surfactant effect during the growth of Li-doped ZnO layers, changing 3D growth to layer-by-layer mode, and proposed that Li atoms on the (000-1) surface lead to a reduction of the surface charge and a decrease of the surface energy.

In our study, we suggest that depolarization could be caused by surface segregation of Ga surfactant. This would change the "forbidden" or "unfavorable" status of the (0001) and (000-1) Tasker-type surfaces, leading to modified polar surfaces that would be more energetically favorable. Indeed, *ab initio* simulations and recent observations by Sohn *et al*. [43] support the modification of surface energies with Ga incorporation. With half monolayer coverage of Ga, they calculate that the surface energy of –C (000-1) is lowered by 1.85 eV whereas +C, M and A surface energies are increased. The role of the electrons given by the Ga atoms is discussed in the framework of the electron counting rule (ECR) : Ga atoms on Zn surface sites would give additional electrons that fill dangling bonds of oxygen surface atoms. This reduction of the polar surface energy is consistent with their experimental work, as they observed, like us, facet and orientation transformations of ZnO nanowires synthesized by vapor phase transport using ZnO:C and GaAs powders as sources. This explanation also fits very well with our own results: (000-1) surface could be energetically favored upon Ga doping, thus explaining the observed stacked bunch of nanoplates.

3.5 Theoretical support on Ga floating behavior

High concentrations of Ga have been measured in our samples. This indicates that Ga atoms may float on the growing surface as surfactants do, but still, a large content is incorporated into the ZnO matrix. This could be due to an incomplete exchange mechanism between Ga and

incoming Zn atoms. A fraction of the Ga atoms on the surface would be buried, probably depending on the TMGa flow and growth conditions.

Northrup *et al*. [44] calculated that indium can float as a stable adlayer on (0001) surface in Zn-rich conditions, and therefore could be used as surfactant. A simple consideration on the formation enthalpies indicates that an oxygen atom will prefer to bind to zinc in order to form ZnO rather than to indium to form In_2O_3. A similar calculation can be made with Ga, considering the formation enthalpies of Ga_2O_3 (-260 kcal/mol) and ZnO (-83kcal/mol), leading to the same conclusion that it is not favorable to form Ga_2O_3. This is confirmed by X-ray diffraction experiments recorded on our GZO samples (not shown here) which never revealed any additional phase of gallium oxide. This suggests that, like indium, Ga atoms could float on the surface as a surfactant.

Finally, to support the floating behavior of Ga atoms and its possible role of surfactant, density functional calculations have been carried out. The ZnO (10-10) M-surface was modelled in a supercell slab geometry consisting of 10 layers of ZnO in a 2×3 surface unit cell (10.6304 Å x 9.8517 Å), including 96 Zn, O or Ga atoms. A vacuum region of 11Å is used (figure 4). The 3 bottom layers are kept fixed during the relaxation to mimic the bulk part. Valence electrons are $2s^2 2p^4$ for oxygen atoms, $3d^{10} 4s^2$ for zinc atoms and $4s^2 4p^1$ for gallium atom. The position of the substitutional Ga_{Zn} dopant has been varied in the ZnO matrix, as illustrated in figure 4 : i) in the bulk, ii) on the topmost surface, and iii) in the atomic plane just below the surface, called "surface-1". Figure 5 shows the computed formation energies of Ga_{Zn} dopant for positions relative to the surface. The results first indicate that negatively charged Ga- ion is the most stable form of the dopant if localized at surface or surface-1, whatever the Fermi level energy. In the bulk, Ga^- ions are only stable when the Fermi level is near the conduction band. One must notice that, whatever the charge or position of the dopant, the distortion of the lattice is weak (*e.g.,* see the distortion

represented for “surface-1” in figure 4, bottom-right), except when the ion is localized on the topmost surface (figure 4, up-right).

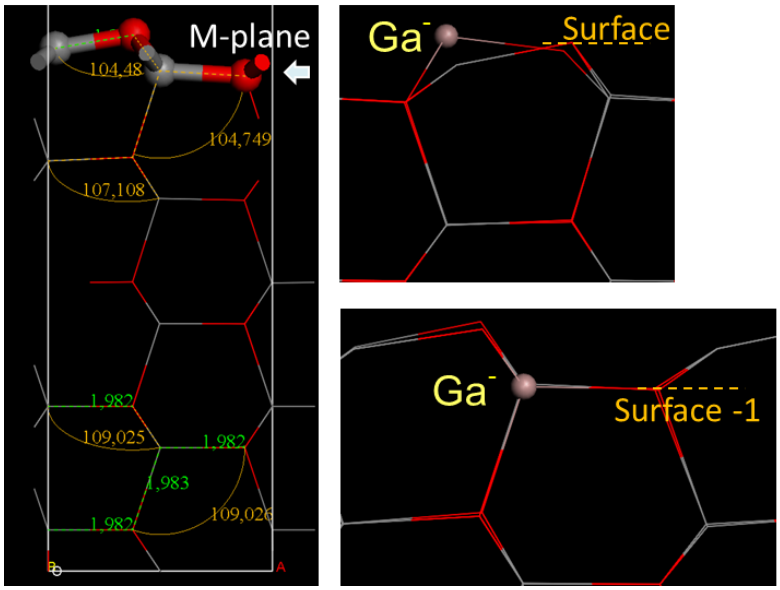

Figure 4. Left) : ZnO supercell slab used for DFT calculations and right) : illustrations of a negatively charged Ga ion localized on the surface or on the atomic plane just below (surface-1)

Therefore, both positions of the Ga atom at surface or surface-1 lead to a decrease of the formation energy, with a value up to – 3eV, compared to the bulk incorporation, as shown in figure 5. These calculations strongly suggest that it is more energetically favorable for Ga to float on the surface, with a negative charge, potentially leading to a surfactant behavior.

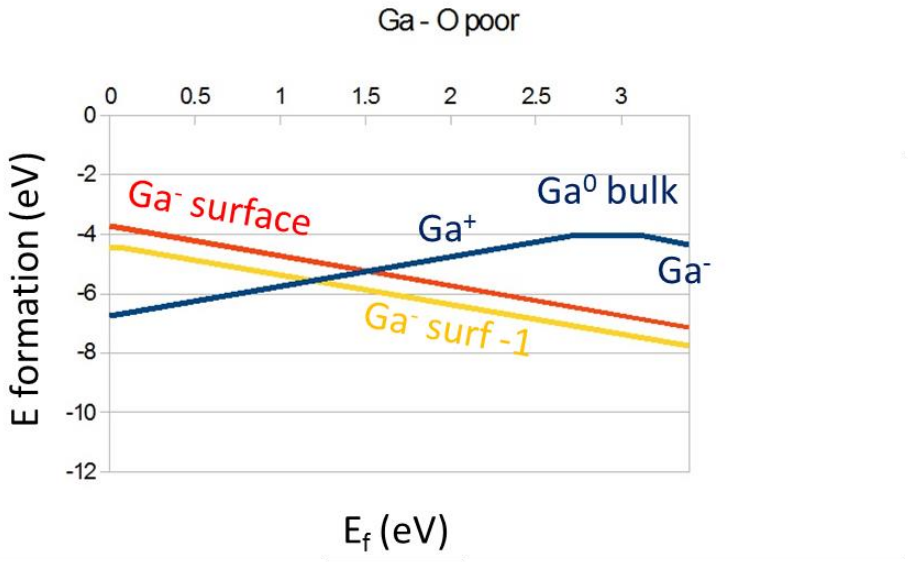

Figure 5. Formation energies of substitutional Ga_{Zn} defects as a function of the Fermi level energy, for different Ga positions: bulk, surface, surface-1

3.6 Optical properties

Optical characterizations, and in particular photoluminescence studies, can give useful information on the presence of dopants, defects, and impurities in the semiconductor matrix. PL measurements have been performed on two sets of samples : i) spontaneous GZO NWs with increasing TMGa flow (non-intentionally doped, 0.03, 0.3 µmol/min), and ii) Au-catalyzed GZO NWs (non-intentionally doped, 0.22, 0.88 µmol/min TMGa). Figure 6a only gathers the spectra of spontaneous GZO NWs but the results for catalyzed GZO NWs are the same (see Supporting Information figure S2). In both cases, the near band edge (NBE) emission and its evolution upon Ga doping is quite similar. For the two types of non-intentionally doped NWs, a sharp transition at 3.358 eV dominates the spectrum with full width at half maximum (FWHM) of ~2 meV. This radiative transition is attributed to Ga donor bound excitons, D°X(Ga), labelled line I_8 [45],

indicating a residual concentration of Ga atoms as a contamination given by the MOCVD reactor (walls, inlet, tubes…). At lower energy, two LO phonon replicas are identified at 3.266 and 3.216 eV. The lines at 3.33 and 3.316 eV can be assigned to excitons related to crystallographic defects (Y line) and to two electron satellite (TES) transition related to Ga donor impurity. It must be noted that before starting Ga doping studies, undoped ZnO 2D films and NWs did not show the D°X emission due to Ga, but rather donor bound excitons due to aluminium at 3.360 eV, labelled line I_6 (see supporting Information, figure S2). These observations evidence the incorporation of Ga and agree with what has been assumed from SIMS measurements. After doping with TMGa (0.03 µmol/min for spontaneous NWs, 0.22 µmol/min for VLS NWs), we clearly observe a blue shift of a few meV associated with a broadening of the D°X(Ga) peak. It is due to the Moss-Burnstein effect and the filling of the electronic states just above the conduction band. This effect, typical of a degenerate semiconductor [46], is further enhanced for the highest TMGa doping flows (0.3 µmol/min for spontaneous NWs, 0.88 µmol/min for VLS NWs), where broad emission bands are measured, indicating a large concentration of Ga donors in the samples.

In order to further assess the presence of free carriers, since direct four-probe measurements are almost impossible on our samples, we turned to photoacoustic (PA) measurements. PA measurements have already been successfully used to probe plasmonic absorption in noble metal-based nanostructures [47,48]. It presents the advantage of providing a clear absorption spectrum without the drawback of a diffuse background as it is generally the case for rough and scattering samples. The photoacoustic signals from the undoped ZnO NWs and the GZO NWs produced with 0.03 µmol/min and 0.3 µmol/min TMGa flows have been recorded and normalized to the Zn-O mode absorption at 500 cm^{-1} (see Supporting Information 3 figure S3). Then, the difference between the PA spectra for the doped NWS and the undoped ones has been plotted, and is shown

in figure 6b. The increase of absorption due to the incorporation of Ga is clearly visible at 1700 cm^{-1}, which would give a plasmonic resonance around 6µm. The peak close to 1000cm^{-1} is related to a difference of absorption between sapphire substrates. These first results confirm both the degenerate character of the NWs and their great potential for mid IR plasmonics.

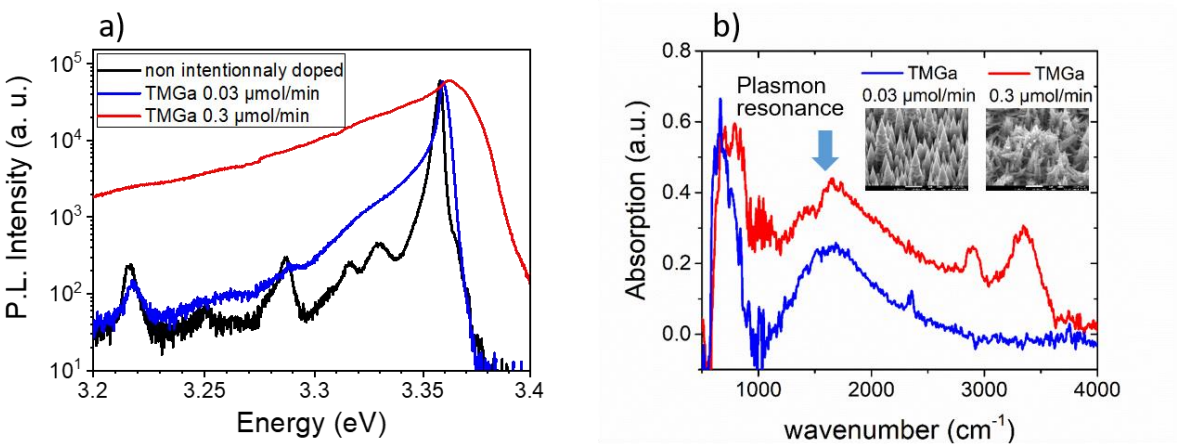

Figure 6. a) PL spectra (T=5K) of spontaneous GZO nanowires with different doping levels, b) normalized absorption spectra of the GZO NWs produced with 0.03µmol/min and 0.3 µmol/min TMGa fluxes, obtained from the difference between the photoacoustic spectra of the doped NWs and the undoped ones

4. CONCLUSION

The influence of TMGa dopant source in the gas phase during the MOCVD growth of ZnO nanowires can be mainly understood by a surfactant effect and the modification of the surface energies and kinetics. The surfactant behavior is supported by DFT calculations. This produces a transformation of the facets of spontaneous GZO NWs, Au-catalyzed GZO NWs, as well as ZnO/ZnO:Ga core-shell structures. In the latter case, this is illustrated by the change of the smooth

initial M-oriented facets that become rougher, with the development of {20-21} surfaces, and further {10-11} surfaces. The morphology evolves progressively towards the appearance of (0001) and/or (000-1) surfaces, which would be stabilized by Ga atoms. However, the surfactant behavior does not fully prevent from Ga incorporation since large concentrations have been measured by RBS and evidenced by PL. In addition, it must be emphasized that a significant surfactant effect occurs even at low Ga concentration in the gas phase due to residual Ga in the MOCVD reactor, and leads to a strong decrease of the NWs aspect ratio. This suggests a kinetic effect involving a reduction of the Zn diffusion length on the lateral facets of the growing nanowire, which would increase the lateral growth rate to the expense of the axial growth rate. Preliminary photoacoustic measurements show an optical absorption at 6 μm and confirm the potential interest of heavily doped ZnO nanostructures for IR plasmonics. These results may also contribute to the construction of metasurfaces and crystal facet engineering in anisotropic ZnO nanostructures, by playing with surface energies to get the desired facet orientation, polarity and/or surface properties. The developed surface could be beneficial to the fabrication of ZnO active devices based on surface reactions, *e.g.,* gas sensors.

FOR TABLE OF CONTENTS USE ONLY

Crystal facet engineering in Ga-doped ZnO nanowires for MIR plasmonics.

Vincent Sallet*, Corinne Sartel, Said Hassani, Christèle Vilar, Gaelle Amiri, Alain Lusson, François Jomard, Pierre Galtier, Isabelle Lefevbre, Christophe Delerue, Mohamed K. Hamza, Bruno Canut, Bruno Masenelli.

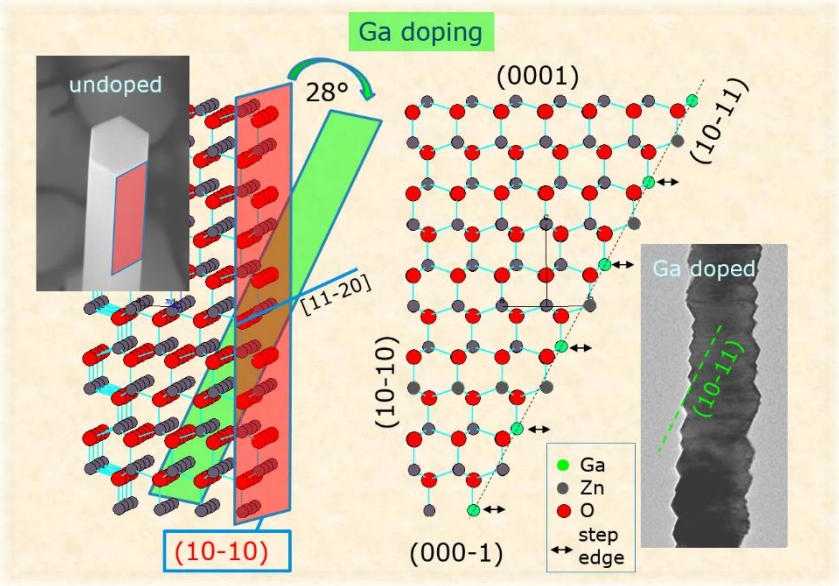

Synopsis

In situ Ga doping during the MOCVD growth of ZnO nanowires induces a change of the smooth initial M-oriented facets, with the subsequent development of {20-21} surfaces, and further {10-11} and {0001} surfaces. A “skewer-like” nanostructure is obtained, exhibiting unusual polar surfaces. The surfactant effect of Ga is discussed. Those Ga-doped nanostructures are suitable for plasmonics in the MIR range.

AUTHOR INFORMATION

Corresponding Author

* vincent.sallet@uvsq.fr

Author Contributions

The manuscript was written through contributions of all authors. All authors have given approval to the final version of the manuscript. ‡These authors contributed equally. (match statement to author names with a symbol)

Funding Sources

This work was supported by the French "Agence Nationale de la Recherche", project n° ANR-15-CE09-0004 (GAZON).

ACKNOWLEDGMENT

B.M. is grateful to Dr. Jaakko Lehtinen from Gasera Company for assistance in the PA measurements. The authors acknowledge the technical staff of the ANAFIRE (Analyses et Faisceaux d'Ions pour la Radiobiologie et l'Environnement) platform at IPNL for their help during the RBS characterizations

SUPPORTING INFORMATION

Detailed descriptions are given as supporting information, including DFT calculations, structural characterization of Au-catalyzed GZO NWs (a TEM image is given in figure S1), and optical characterizations (PL spectra of undoped ZnO NWs and Au-catalyzed GZO NWs are shown in figure S2, raw photoacoustic signals in figure S3). Supporting information is available free of charge via the Internet at http://pubs.acs.org/.

IN MEMORIAM

The authors would like to dedicate this article to the memory of Prof. Dr. Pierre Galtier, departed too early.

REFERENCES

[1] Lu, W.; Leiber, C.M. Semiconductor nanowires. *J. Phys. D: Appl. Phys.* **2006**, 39, R387-R406.
[2] Barth, S.; Hernandez-Ramirez, F.; Holmes J.D.; Romano-Rodriguez, A. Synthesis and applications of one-dimensional semiconductors. *Progress in Materials Science* **2010**, 55, 563-627.
[3] Consonni, V.; Feuillet, G. Wide Band Gap Semiconductor Nanowires 2: Heterostructures and Optoelectronic Devices. *WILEY-ISTE* **2014**.
[4] Look, D.C.; Leedy, K.D. ZnO plasmonics for telecommunications. *Appl. Phys. Lett.* **2013**, 102, 182107.
[5] Sadofev, S.; Kalusniak, S.; Shafer, P.; Henneberger, F. Molecular beam epitaxy of n-Zn(Mg)O as a low-damping plasmonic material at telecommunication wavelengths. *Appl. Phys. Lett.* **2013**, 102, 181905.
[6] Hamza, M.K.; Bluet, J.-M.; Masenelli-Varlot, K.; Canut, B.; Boisron, O.; Melinon P.; Masenelli, B. Tunable mid IR plasmon in GZO nanocrystals. *Nanoscale* **2015**, 7, 12030-12037.
[7] Li, S. Q.; Guo, P.; Zhang, L.; Zhou, W.; Odom, T. W.; Seideman, T.; Ketterson, J. B.; Chang, R. P. H. Infrared Plasmonics with Indium–Tin-Oxide Nanorod Arrays. ACS Nano **2011**, 5, 9161–9170.
[8] Liu, G.; Yu, J.C.; Lu, G.Q.; Cheng, H.-M. Crystal facet engineering of semiconductor photocatalysts: motivations, advances and unique properties. *Chem. Commun.* **2011**, 47, 6763–6783
[9] Verrier, C.; Appert, E.; Chaix-Pluchery, O.; Rapenne, L.; Rafhay, Q.; Kaminski-Cachopo, A.; Consonni, V.; Tunable Morphology and Doping of ZnO Nanowires by chemical Bath Deposition Using Aluminum Nitrate. *J. Phys. Chem. C* **2017**, 121, 3573-3583
[10] Fan, H. J.; Fuhrmann, B.; Scholz, R.; Himcinschi, C.; Berger, A.; Leipner, H.; Armin Dadgar; Krost, A.; Christiansen, S.; Gösele, U.; Zacharias, M. Vapour-transport-deposition growth of ZnO nanostructures: switch between c -axial wires and a -axial belts by indium doping. *Nanotechnology* **2006**, 17, S231-S239.
[11] Sharma, S.; Sharma, Y.; Sharma, J. Synthesis and characterization of ZnO flower-like structures. *Smart Science* **2016**, 4, 8–13.
[12] Pal, K.; Zhan, B.; Ma, X.; Wang, G.; Schirhagl, R.; Murgasen, P. Optical and Electrical Investigation of ZnO Nano-Wire Array to Micro-Flower from Hierarchical Nano-Rose Structures. J. Nanosci. Nanotechnol. **2016**, 16, 400-409.

[13] Mayer M. SIMNRA Users Guide, *Max-Plank-Institut für Plasmaphysik Technical Report* **1997** N°. IPP9/113

[14] Montenegro, D. N.; Souissi, A.; Martínez-Tomás, C.; Muñoz-Sanjosé, V.; Sallet, V. Morphology transitions in ZnO nanorods grown by MOCVD. *Journal of Crystal Growth* **2012**, 359, 122–128.

[15] Blöchl, P. E. Projector augmented-wave method. *Phys. Rev. B* **1994**, 50, 17953–17979.

[16] Kresse, G.; Furthmüller, J. Efficiency of ab-initio total energy calculations for metals and semiconductors using a plane-wave basis set. *Computational Materials Science* **1996**, 6, 15–50.

[17] Rosina, M.; Ferret, P.; Jouneau, P.-H.; Robin, I.-C.; Levy, F.; Feuillet, G.; Lafossas, M. Morphology and growth mechanism of aligned ZnO nanorods grown by catalyst-free MOCVD. *Microelectronics Journal* **2009**, 40, 242–245.

[18] Behrends, A.; Bakin, A.; Waag, A. Investigation of ZnO nanopillars fabrication in a new Thomas Swan close coupled showerhead MOCVD reactor. *Microelectronics Journal* **2009**, 40, 280–282.

[19] Perillat-Merceroz, G.; Thierry, R.; Jouneau, P.-H.; Ferret, P.; Feuillet, G. Compared growth mechanisms of Zn-polar ZnO nanowires on O-polar ZnO and on sapphire. *Nanotechnology* **2012**, 23, 125702.

[20] Ren, Z.; Guo, Y.; Liu, C.-H.; Gao, P.-X. Hierarchically nanostructured materials for sustainable environmental applications. *Frontiers in Chemistry* **2013**, 1, 18.

[21] (1) Wagner, R. S.; Ellis, W. C. Vapor-liquid-solid mechanism of single crystal growth. *Applied Physics Letters* **1964**, 4, 89–90.

[22] Gottschalch, V.; Wagner, G.; Bauer, J.; Paetzelt, H.; Shirnow, M. VLS growth of GaN nanowires on various substrates. *Journal of Crystal Growth* **2008**, 310, 5123–5128.

[23] Diebold, U.; Koplitz, L. V.; Dulub, O. Atomic-scale properties of low-index ZnO surfaces. *Applied Surface Science* **2004**, 237, 336–342.

[24] Kandel, D.; Kaxiras, E. Surfactant Mediated Crystal Growth of Semiconductors *Phys. Rev. Lett.* **1995**, 75, 2742–2745.

[25] Kaxiras, E. Atomic structure of surfactant monolayers and its role in epitaxial growth *Materials Science and Engineering: B* **1995**, 30, 175–186.

[26] Ye, J. D.; Tan, S. T.; Pannirselvam, S.; Choy, S. F.; Sun, X. W.; Lo, G. Q.; Teo, K. L. Surfactant effect of arsenic doping on modification of ZnO (0001) growth kinetics. *Applied Physics Letters* **2009**, 95, 101905.

[27] Harmand, J. C.; Li, L. H.; Patriarche, G.; Travers, L. GaInAs/GaAs quantum-well growth assisted by Sb surfactant: Toward 1.3 μm emission. *Applied Physics Letters* **2004**, 84, 3981–3983.

[28] Neplokh, V.; Messanvi, A.; Zhang, H.; Julien, F. H.; Babichev, A.; Eymery, J.; Durand, C.; Tchernycheva, M. Substrate-Free InGaN/GaN Nanowire Light-Emitting Diodes. *Nanoscale Research Letters* **2015**, 10, 447

[29] Yang, Z.; Han, N.; Fang, M.; Lin, H.; Cheung, H.-Y.; Yip, S.; Wang, E.-J.; Hung, T.; Wong, C.-Y.; Ho, J. C. Surfactant-assisted chemical vapour deposition of high-performance small-diameter GaSb nanowires. *Nature Communications* **2014**, 5, 5249.

[30] Zhang, L.; Tang, H. F.; Kuech, T. F. Effect of Sb as a surfactant during the lateral epitaxial overgrowth of GaN by metalorganic vapor phase epitaxy. *Applied Physics Letters* **2001**, 79, 3059–3061.

[31] Voigtländer, B.; Zinner, A.; Weber, T.; Bonzel, H. P. Modification of Growth Kinetics in Surfactant-Mediated Epitaxy. Phys. Rev. B **1995**, 51, 7583–7591.

[32] Wöll, C. The Chemistry and Physics of Zinc Oxide Surfaces. *Progress in Surface Science* **2007**, 82, 55–120.

[33] Goniakowski, J.; Finocchi, F.; Noguera, C. Polarity of Oxide Surfaces and Nanostructures. *Reports on Progress in Physics* **2008**, 71, 016501.
[34] Zúñiga-Pérez, J.; Consonni, V.; Lymperakis, L.; Kong, X.; Trampert, A.; Fernández-Garrido, S.; Brandt, O.; Renevier, H.; Keller, S.; Hestroffer, K.; et al. Polarity in GaN and ZnO: Theory, Measurement, Growth, and Devices. *Applied Physics Reviews* **2016**, 3, 041303.
[35] Tasker, P. W. The stability of ionic crystal surfaces. *Journal of Physics C: Solid State Physics* **1979**, 12, 4977.
[36] Meyer, B.; Marx, D. Density-functional study of the structure and stability of ZnO surfaces *Phys. Rev. B* **2003**, 67, 035403.
[37] Wander, A.; Schedin, F.; Steadman, P.; Norris, A.; McGrath, R.; Turner, T. S.; Thornton, G.; Harrison, N. M. Stability of Polar Oxide Surfaces *Phys. Rev. Lett.* **2001**, 86, 3811–3814.
[38] Kunat, M.; Gil Girol, S.; Becker, T.; Burghaus, U.; Wöll, C. Stability of the polar surfaces of ZnO: A reinvestigation using He-atom scattering. *Phys. Rev. B* **2002**, 66, 081402.
[39] Kresse, G.; Dulub, O.; Diebold, U. Competing stabilization mechanism for the polar ZnO(0001)-Zn surface. *Phys. Rev. B* **2003**, 68, 245409.
[40] Dulub, O.; Diebold, U.; Kresse, G. Novel Stabilization Mechanism on Polar Surfaces: ZnO(0001)-Zn. *Phys. Rev. Lett.* **2003**, 90, 016102.
[41] Lauritsen, J. V.; Porsgaard, S.; Rasmussen, M. K.; Jensen, M. C. R.; Bechstein, R.; Meinander, K.; Clausen, B. S.; Helveg, S.; Wahl, R.; Kresse, G.; Besenbacher, F. Stabilization Principles for Polar Surfaces of ZnO. *ACS Nano* **2011**, 5, 5987–5994.
[42] Yuan, H. T.; Zeng, Z. Q.; Mei, Z. X.; Du, X. L.; Jia, J. F.; Xue, Q. K. Surfactant effects of lithium dopant during molecular beam epitaxy of ZnO films *Journal of Physics: Condensed Matter* **2007**, 19, 482001.
[43] Sohn, J. I.; Hong, W.-K.; Lee, S.; Lee, S.; Ku, J.; Park, Y. J.; Hong, J.; Hwang, S.; Park, K. H.; Warner, J. H.; Cha, S.; Kim, J. M. Surface energy-mediated construction of anisotropic semiconductor wires with selective crystallographic polarity. *Scientific Reports* **2014**, 4, 5680.
[44] Northrup, J. E.; Neugebauer, J. Metal-adlayer-stabilized ZnO(0001) surfaces: Toward a new growth mode for oxides *Applied Physics Letters* **2005**, 87, 141914.
[45] Meyer, B. K.; Alves, H.; Hofmann, D. M.; Kriegseis, W.; Forster, D.; Bertram, F.; Christen, J.; Hoffmann, A.; Straßburg, M.; Dworzak, M.; Haboeck, U.; Rodina, A. V. Bound exciton and donor–acceptor pair recombinations in ZnO. *Physica status solidi (b)* **2004**, 241, 231–260.
[46] Park, H. C.; Byun, D.; Angadi, B.; Park, D. H.; Choi, W. K.; Choi, J. W.; Jung, Y. S. Photoluminescence of Ga-doped ZnO film grown on c-Al2O3 (0001) by plasma-assisted molecular beam epitaxy. *Journal of Applied Physics* **2007**, 102, 073114.
[47] Inagaki, T.; Kagami, K.; Arakawa, E. T. Photoacoustic study of surface plasmons in metals. *Appl. Opt.* **1982**, 21, 949–954.
[48] El-Brolossy, T. A.; Abdallah, T.; Mohamed, M. B.; Abdallah, S.; Easawi, K.; Negm, S.; Talaat, H. Shape and size dependence of the surface plasmon resonance of gold nanoparticles studied by Photoacoustic technique. *The European Physical Journal Special Topics* **2008**, 153, 361–364.